*Transactions*, **SMiRT-26**
**Berlin/Potsdam, Germany, July 10-15, 2022**
**Division I**

# TESTING AND ANALYSIS OF HELICAL SPRING COMPONENTS TO EVALUATE THE EFFECT OF EXPOSURE TO REACTOR CONDITIONS ON MATERIAL PROPERTIES

**Donald Metzger[1], Andre Gagnon[2], Tejasvi Kashyap[3] and Razvan Vidican[4]**

[1]Principal Engineer, SNC-Lavalin Nuclear (Candu Energy Inc.), Mississauga Ontario Canada (Don.Metzger@snclavalin.com)
[2] Engineer, SNC-Lavalin Nuclear (Candu Energy Inc.), Mississauga Ontario Canada (Andre.Gagnon2@snclavalin.com)
[3]Analyst, SNC-Lavalin Nuclear (Candu Energy Inc.), Mississauga Ontario Canada
[4]Specialist Engineer, SNC-Lavalin Nuclear (Candu Energy Inc.), Mississauga Ontario Canada

## ABSTRACT

Testing and analysis of helical spring components is required to evaluate the impact of exposure to reactor conditions on material properties. Assessment of the spring integrity requires data about material degradation for both static load capacity and fatigue performance. Customized tests were developed to obtain information on static and fatigue performance of Inconel X-750 springs and, in combination with analysis, can be used to estimate material properties. The static and fatigue test methods are presented along with irradiated and unirradiated test results. The test results are compared with analysis and alternate data to demonstrate the quality of the test data and the practicality of using these test methods for assessing the material. The tests methods are found to produce high quality test data for both unirradiated and irradiated material.

## INTRODUCTION

In many nuclear reactors in Canada, separation between two structural components is maintained by spacers made of helical springs such that the separating load bears across the diameter of the spring coils. The loading in service is generally quasi-static, but relative motion between the structural components due to pressure and temperature transients as well as creep deformation is accommodated by rolling of the spring. This rolling motion while under radial load causes cyclic stress in the spring material such that evaluation of the spring's integrity must consider fatigue usage as well as the static load capacity. The small size of coil diameter and cross section of the spring precludes the use of standard test methods so specialized tests have been developed. Two separate test systems address quasi-static loading and fatigue loading respectively (See Metzger, Gagnon, Kashyap and Vidican (2021)). In both cases, the loading primarily results in bending stress which is generally consistent with the stress caused by loading of the component in service.

The helical spring in the spacer in made of Inconel alloy X-750. The wire that is coiled to make the spring is nominally square but there is variability in the geometry that must be considered in subsequent analysis to accurately estimate the stress state in the spring. Mainly, the cross section of the wire can show variation in corner rounding as well as difference of the height and width of the wire. The material is primarily composed of Nickle and is known to experience significant material property changes when exposed to neutron irradiation. The irradiation conditions are in a dry environment with a high proportion of thermal neutrons. A spacer in the installed configuration can be seen in Figure 1 along with examples

of typical test specimens. The load bearing part of the spring is at the bottom of Figure 1 where the weight of the fuel, coolant and pressure tube pinches the spacer against the calandria tube.

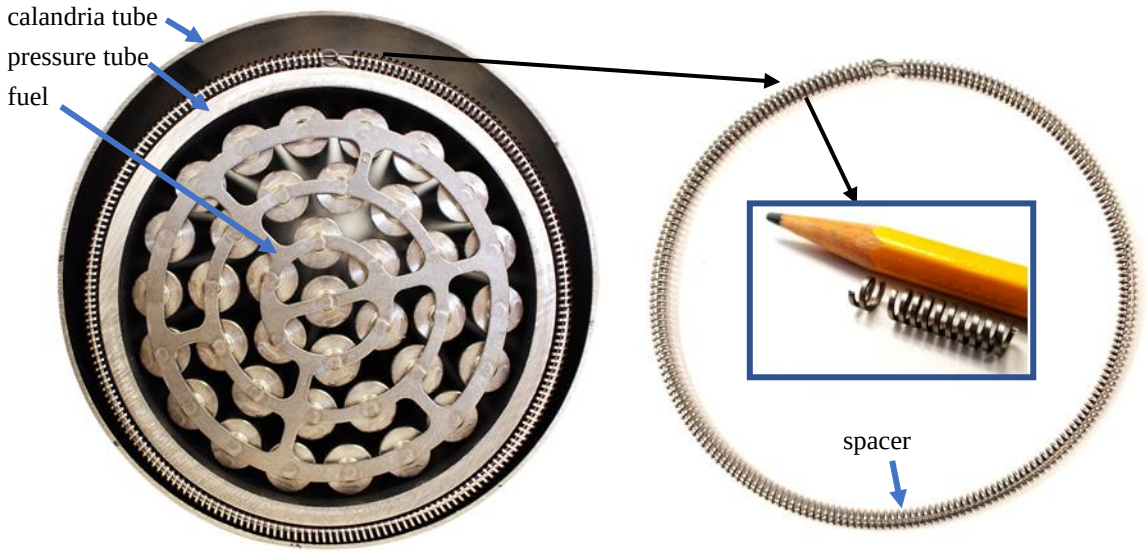


Figure 1. Spacer in the installed configuration and a spacer with example test specimens

## MULTI-COIL CRUSH TEST

One method of determining the material properties is to test a short piece of spring by compressing it radially. The specimen is typically composed of at least 10 coils to lessen the influence of the free end condition on the load-displacement curve. The specimen is placed between two rigid flat platens and is compressed radially at a constant rate of displacement. An image of a specimen in the test system can be seen in Figure 2. The load is measured by a load cell behind one of the platens and the displacement is measured using a linear variable displacement transducer on each side of the specimen. This is a simple method of testing the material and produces useful data but there are some complications that must be considered when analysing the results.

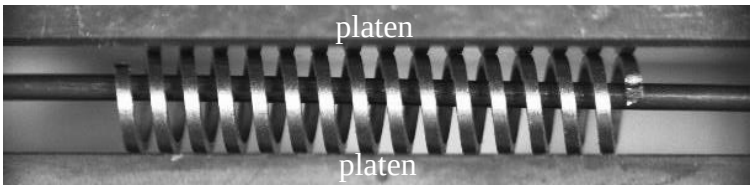


Figure 2. Multi-coil crush test specimen during a test

One benefit of the multi-coil crush test is that the loading condition is similar to that seen in the reactor. This loading condition stresses the coil predominantly due to bending and the resulting bending stress distribution in the coils is shown in Figure 3. However, as shown in Figure 3, there is only a small region of the coil that is subjected to high stress and the stress varies at different locations in a coil; this complicates extraction of material data. The analysis is further complicated by variability of coil diameters and uncertainty in the contact condition between the coils and the platens. The friction associated with the contact condition is also challenging to estimate, but accurate estimates of friction for the irradiated specimens are needed to reduce uncertainty. The impact of the contact condition on the responses of the spring is highlighted in Figure 4 which shows finite element results of crush testing and demonstrate how

the load-displacement curve changes for different levels of friction. Some test results were analysed for unirradiated spacers, see Metzger, Gagnon, Kashyap (2021), which use specimens of different length to estimate the friction, but this was not practical for the irradiated springs.

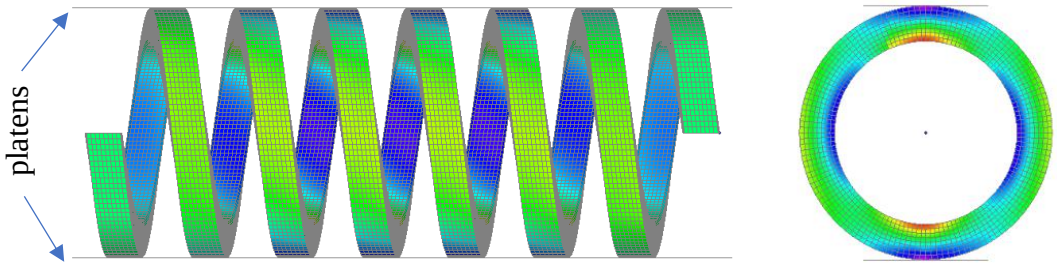


Figure 3. Bending stress distribution in multi-coil crush test specimen (right image is for a central coil)

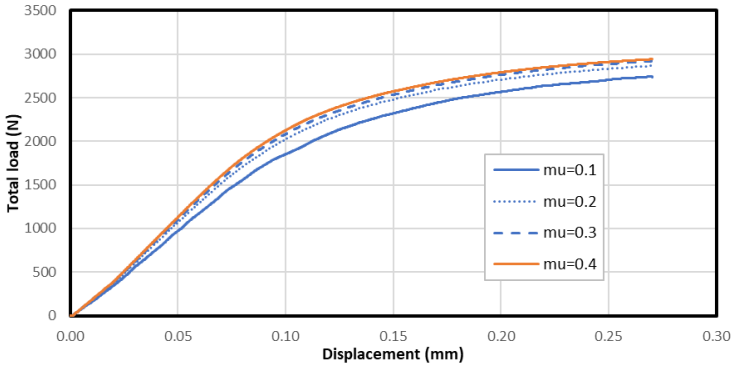


Figure 4. Finite element multi-coil load versus displacement curves at different levels of friction

An incorrect estimate of friction can result in significant errors in relating the coil load capacity to material property estimates. A new method to estimate the friction coefficient was employed for the irradiated specimens which took advantage of high-resolution photographs taken during the test; an example photograph can be seen in Figure 2. A lower friction will result in a larger amount of displacement of the end coils since there is insufficient tangential contact force to prevent the end coil from sliding against the platens. The photographs recorded throughout the test can be used to measure the coil displacement. The vertical displacement for a finite element model at two different levels of friction can be seen in Figure 5 and clearly show that the last coil displaces more at lower levels of friction.

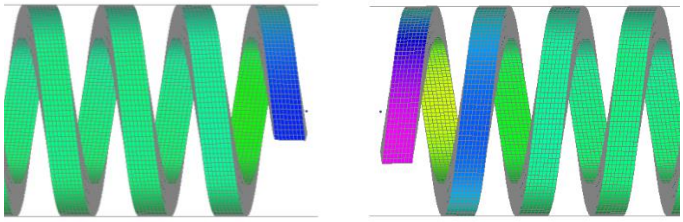

Figure 5. Vertical displacement of end coils relative to coil centre for friction of 0.2 (left) and 0.1 (right)

The local displacement of the coils was tracked throughout the test and output at a common set of platen displacements before the specimens yielded. This method was only possible where the end coils had material near the centre of the platen because the component of the coil displacement perpendicular to the

camera view needed to be sufficiently large for accurate estimates. This method was used to measure the coil displacement of numerous irradiated and unirradiated specimens. The results of these measurements have been plotted against the displacement estimates for the corresponding coils from finite element models with different levels of friction in Figure 6. The results show that there is variability of the friction estimates for any given test, but on average the irradiated and unirradiated specimens have a very similar level of friction. This variability is not unexpected and is due in part from measurement error and in part from variability of the coil outer diameters which will change the response of the spring.

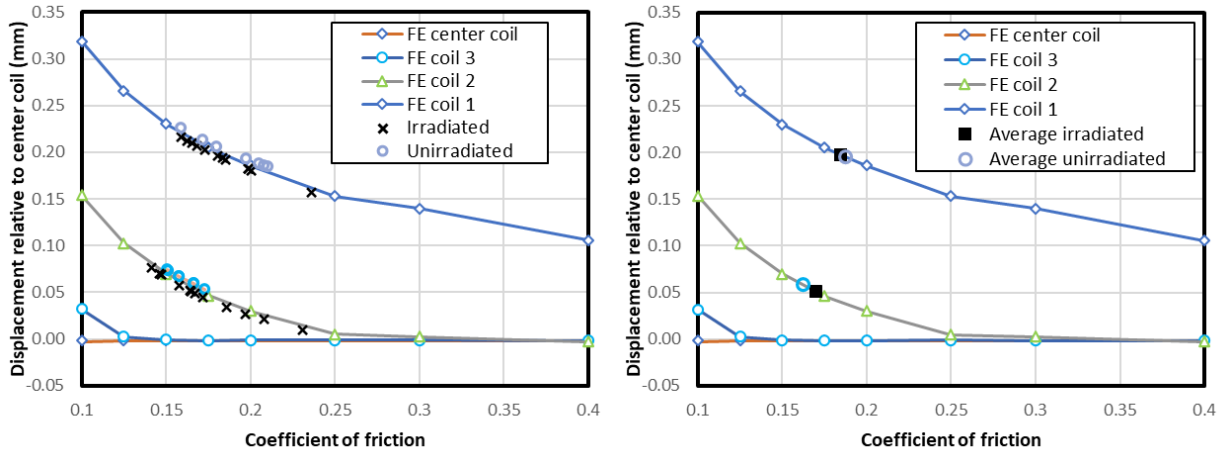


Figure 6. Vertical deflection of end coils comparing test data with finite element models

Because the friction is similar between the irradiated and unirradiated specimens, it is possible to the directly compare the test results from an irradiated and unirradiated specimen with similar dimensions. An irradiated an unirradiated load-displacement curve can be seen in Figure 7. The irradiated test in Figure 7 is for a specimen with very low ductility which is not uncommon for this irradiated material. Examining the graph closely, it is possible to see where the two crush curves separate, and these small differences can be analysed to estimate the changes in material properties. The example of Figure 7 indicates that irradiation has increased yield stress but lowered ductility. With knowledge of the friction and specimen dimensions, there is sufficient information to estimate material properties from the crush test data. Using analytical equation along with detailed finite element analysis it was possible to obtain good estimates of the material properties of the irradiated specimens using multi-coil crush test results.

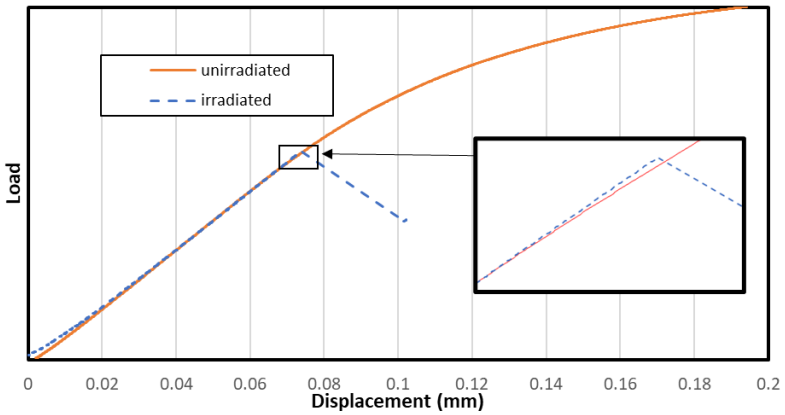


Figure 7. Comparison of test data for an irradiated and unirradiated multi-coil crush test

## SINGLE COIL CRUSH TEST

A new test method using a single coil was developed to address some of the challenges associated with estimating material properties using the multi-coil crush tests. One advantage of using a single coil for a test is that a smaller test specimen allows more test data to be obtained from a spring and given the cost of obtaining ex-service material this is very important. The new test method uses a similar testing approach as the multi-coil crush test in that a piece of spring is compressed radially, but instead of testing many coils a single coil of approximately 1.5 turns is tested. A photograph of the single coil in the test rig can be seen in Figure 8. The single coil test eliminates uncertainty due to the coil-to-coil variability of the wire dimension and outer diameter that is present for multi-coil test specimens. Additionally, this test method employs a fine-toothed precision file as a high friction surface to prevent sliding of the coil; this eliminates the uncertainty associated with the contact condition between the platen and the specimen. The single coil test also required additional constraints to prevent coil rotation as shown in the finite element model in Figure 9. These constraints were incorporated into the test system since they are necessary to control the response of the test specimen to achieve the most appropriate stress state. The bending stress in the coil is shown in right image in Figure 9 with the extra constraints removed from view.

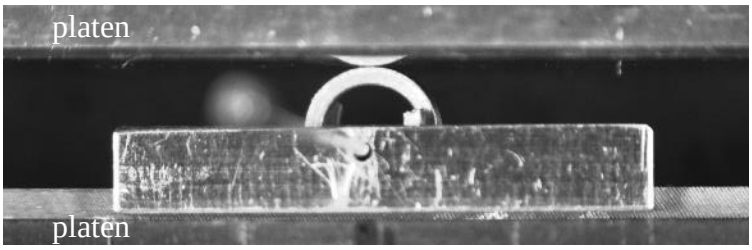


Figure 8. Single coil specimen installed in the test rig

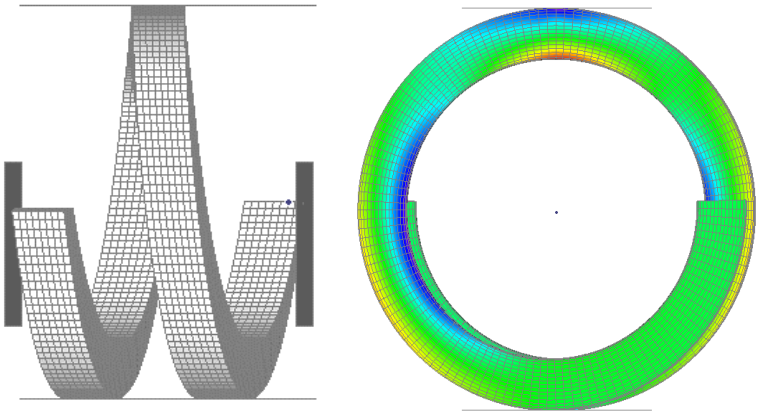

Figure 9. Single coil specimen constraints and bending stress in single coil specimen

The test results from the single coil specimens were found to be very consistent and repeatable. An example of load-displacement curves from 7 unirradiated tests are shown in Figure 10 along with a finite element load-displacement curve based on results presented in Gagnon, Metzger and Kashyap (2021). The similarity of the load-displacement data from the test and the finite element results confirmed that the unirradiated specimens could be adequately tested and analysed to estimate material properties. The results also confirm that the combination of end supports and control of the sticking friction contact condition using a file were sufficient to control the coil as intended. All unirradiated specimens deformed plastically and the tests were stopped at relatively low displacement with no fracture of the of the coil.

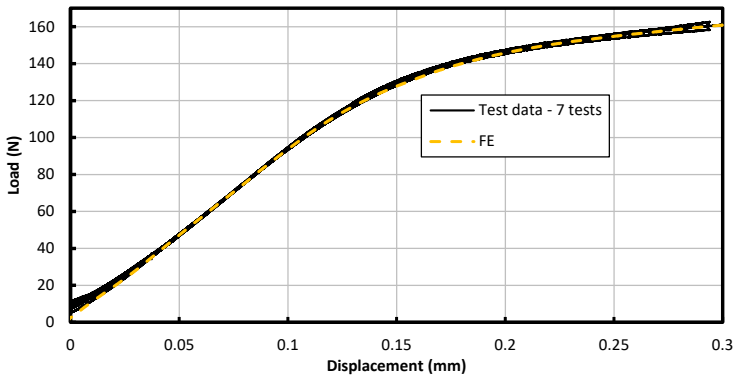


Figure 10. Load versus displacement of 7 unirradiated single coil tests and finite element results

The single coil crush test was also used on irradiated specimens. A total of three irradiated single coil specimens were tested until failure with two results very consistent and a third result within the variability that would be expected for a multi-coil crush test. All specimens fractured in the highly stressed regions near the top and sides of the coil and a photograph of a specimen shortly after fracture can be seen in Figure 11. The load displacement curves for the two consistent specimens are shown in Figure 12 (from Gagnon, Metzger and Kashyap (2021)). One crush curve shows lower strength and more ductility, and this was expected for some specimens since some coils operate at lower temperature and material irradiated at lower temperatures tends to exhibit more ductile behaviour. The differences in material properties were confirmed using a finite element model which had two different stress strain curves but identical geometry. As can be seen in Figure 12 the analysis results match the test data very well and confirm that the test data can be compared against analysis to estimate the properties of the irradiated material.

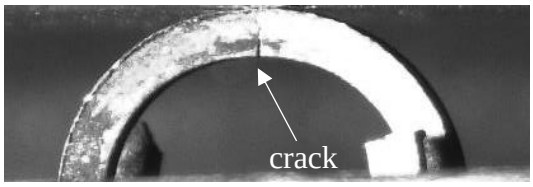


Figure 11. Crack in irradiated single coil specimen after testing

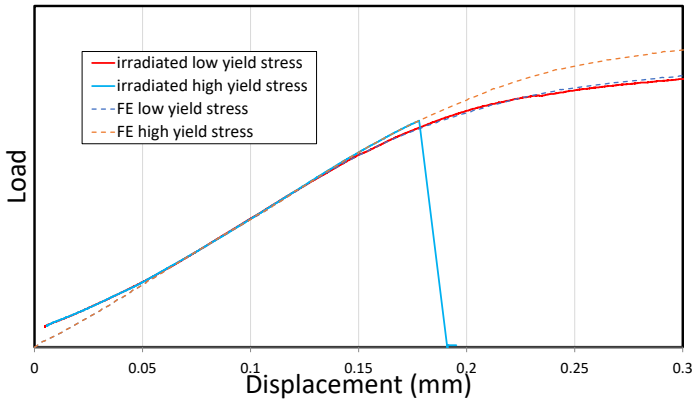


Figure 12. Comparison of two irradiated spacer tests with finite element analysis from models with identical geometry

## TORSION FATIGUE TEST

A third type of test was used to determine the fatigue properties of the spring material. The test is performed using a short section of spring approximately 14 coils long. Inside each end of the specimen a properly sized mandrel is inserted with specific profile to prevent stress concentration in the specimen from promoting premature failure. The specimen ends are then inserted into collets and the collets clamp the spacer against the mandrel for approximately 2 coils on each end. A specimen installed in the test rig with the various parts labelled can be seen in Figure 13. With the specimen held at both ends, one end is kept stationary and attached to a load cell while the other end is rotated using a motor with a sinusoidally applied torque. This test method put the specimen into pure bending and the entire outer circumference and inner circumference of the specimen is subjected to high stress; this can be seen in Figure 14.

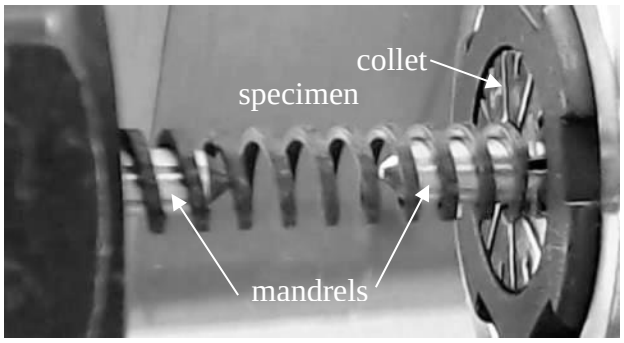


Figure 13. Specimen installed in fatigue test rig

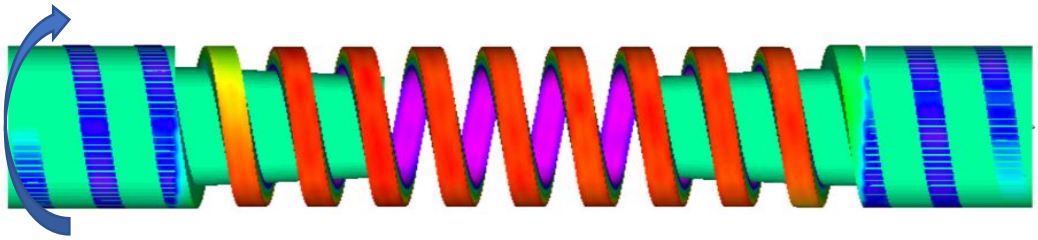

Figure 14. Bending stress in torsion fatigue specimen (red is tensile and purple compressive)

Some results for unirradiated specimens have been presented in Gagnon, Kashyap and Metzger (2021). The specimens behaved very consistently with all fatigue cracks starting on the inner diameter of the coil where the stress amplitude is slightly higher due to curved bar mechanics. An example of the fracture surface for an unirradiated specimen can be seen in Figure 15 which shows fatigue striations occurring from a crack initiating on the inner diameter of the coil. After completion of the tests a small amount of plastic deformation was used to bend the coil and numerous cracks could be seen at low magnification along the specimen inner diameter. This provides good evidence that the stress is applied uniformly along the length of the specimen. Numerous unirradiated specimens were tested to failure and are plotted against the fatigue curve for a similar material from Jaske and O'Donnell (1977) in Figure 16. The stress amplitude for the torsion specimen was estimated using curved beam theory which agreed well with the finite element modelling. The test method for the Inconel 718 material in Figure 16 was generated in a very different way but the results for the current material are very similar and this gives high confidence the test method is functioning properly for the unirradiated material.

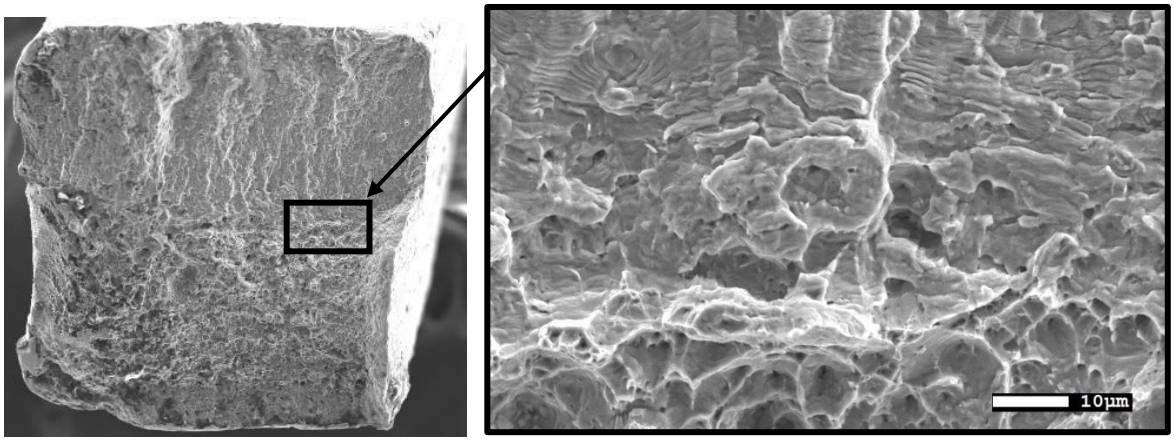


Figure 15. Scanning electron microscope images of fracture surface of unirradiated fatigue specimen

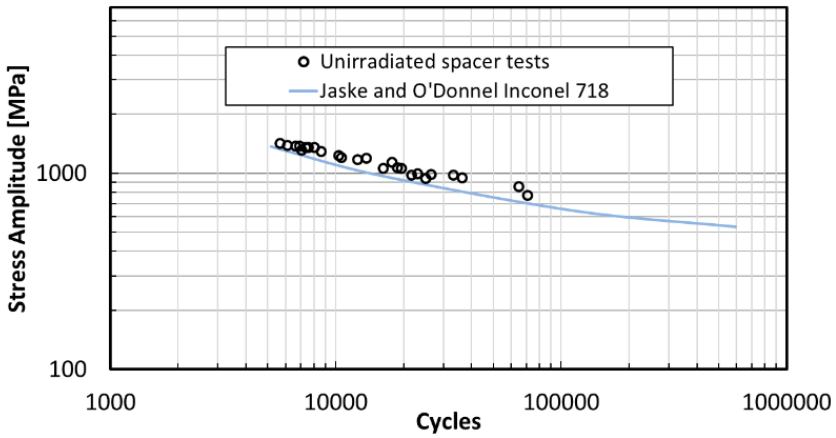


Figure 16. Test data of unirradiated spacers compared to a fatigue curve of similar material

The torsion fatigue test system was used to test irradiated springs and the test method functioned properly resulting in all specimens failing due to cracks propagating from the inner diameter of the specimen. In all cases the specimens failed in locations free of any support from the grips, and two images of typically irradiated specimens after failure can be seen in Figure 17. An example of a fracture surface from an irradiated fatigue test can be seen in Figure 18. There was a small region of the fracture surface near the inner diameter that was different from the typical intragranular failure of this material and shows some evidence of striations in higher magnification images.

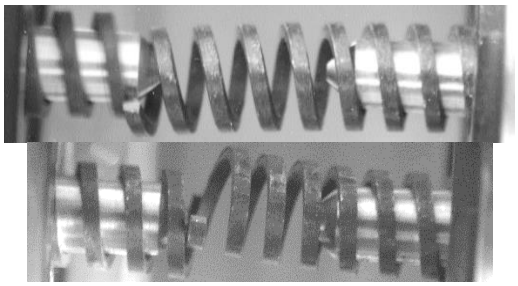

Figure 17. Two irradiated specimens after fracture during torsion fatigue test

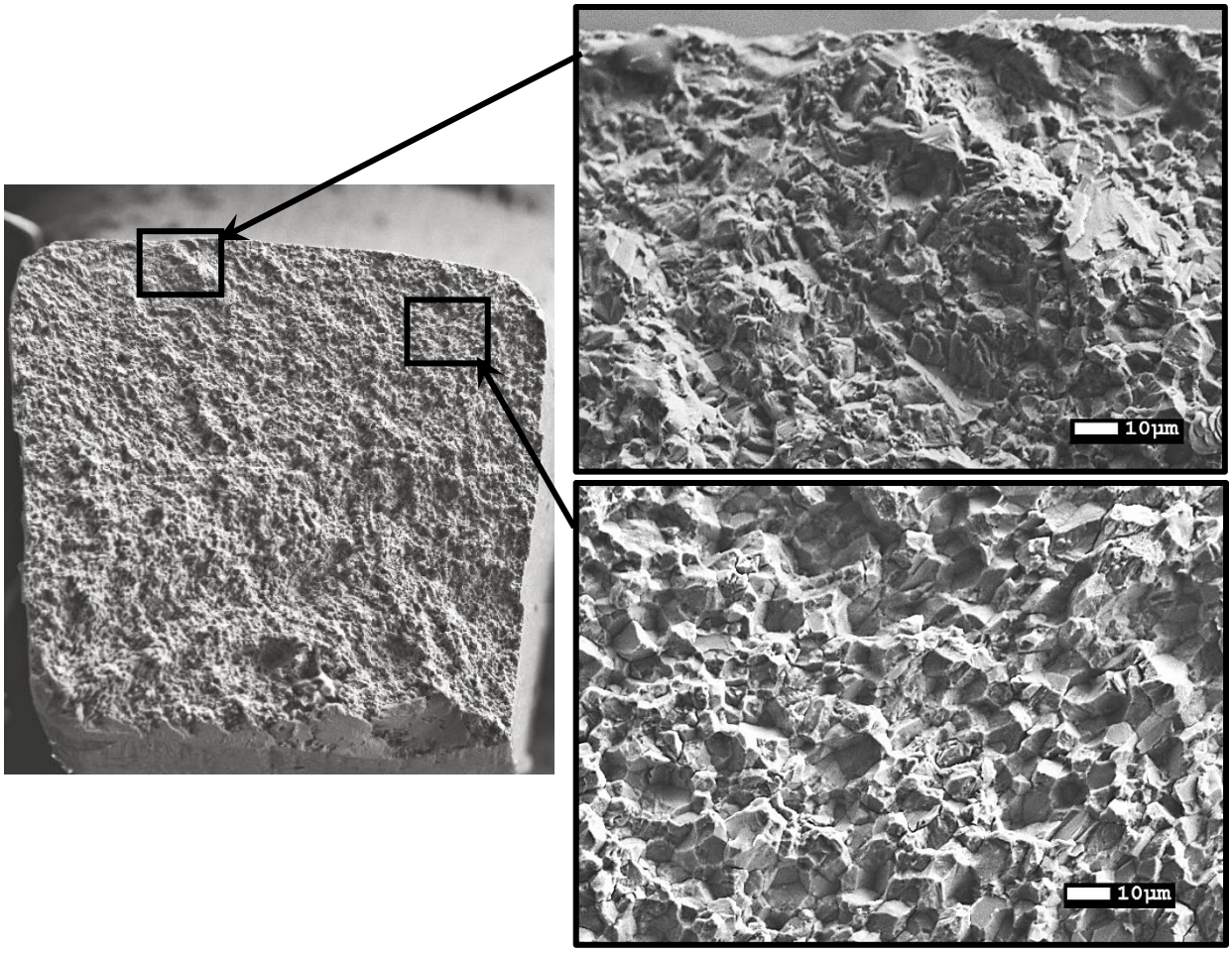


Figure 18. Fracture surface of irradiated fatigue specimen showing atypical region near inner diameter and intergranular fracture typical of the rest of the fracture surface.

The torsion test rig also recorded the rotation of the motor that was rigidly attached to the end of the specimen. The rotation of an unirradiated and irradiated specimen plotted versus the cycles can be seen in Figure 19. Because the test rig applied torque sinusoidally with a nominally constant amplitude, the rotation can be used to observe changes of the specimen stiffness. As shown in Figure 19, the rotation of the unirradiated specimen increases as test progresses which is an indication of reduced specimen stiffness that is caused by the propagation of fatigue cracks. The blue curve for the irradiated specimen shown in Figure 19 demonstrates that there is little to no reduction in stiffness prior to failure. This was expected because of the low ductility of the material and this provides more evidence that the material did not allow significant fatigue crack propagation prior to fast fracture. This observation of specimen rotation was consistent for all unirradiated and all irradiated specimens. The torsion test method performed well with the irradiated specimens and generated good quality fatigue data that can be used to generate a fatigue curve for the irradiated material.

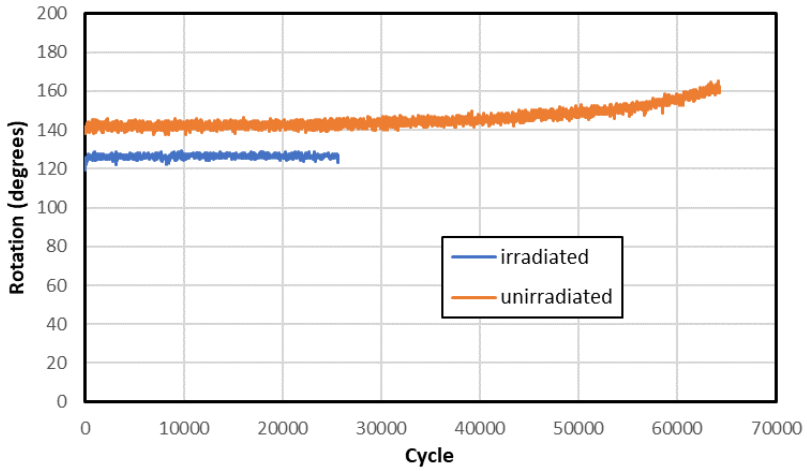


Figure 19. Rotation of an irradiated and unirradiated fatigue specimen during the torsion fatigue test

## CONCLUSION

Three test methods were used to obtain test data from unirradiated and irradiated springs made of Inconel X-750. The results from all three test methods were in good agreement with analysis. The test methods worked equally well of irradiated and unirradiated material and these test methods in combination with analysis are suitable for obtaining material properties for helical springs.

## ACKNOWLEDGMENTS

The scanning electron microscopy and irradiated spacer work was performed at the Korea Atomic Energy Research Institute (KAERI). We would specifically like to thank YoungJun Kim, SukWoo Hong, YoungGwan Jin, JinHo Park, BoungOk Yoo, YangHong Jung and KiSoo Heo for their significant contribution and expertise in performing the sample preparation, testing and material characterization.

## REFERENCES

Gagnon, A., Kashyap, T., Metzger, D.R. (2021), *Torsional Fatigue Test Applicable to Helical Spring Material Used in CANDU Fuel Channel Spacers*, Proceedings of the ASME 2021 Pressure Vessels and Piping Conference, Virtual.

Gagnon, A., Metzger, D.R., Kashyap, T. (2021*), Single Coil Tests of Ex-Service Inconel X-750 Fuel Channel Annulus Spacers*, Canadian Nuclear Society 2nd International Conference on Materials, Chemistry and Fitness-For-Service Solutions, Virtual.

Jaske, C.E., and W.J. O'Donnell, (1977) *Fatigue Design Criteria for Pressure Vessel Alloys*, Transactions of the ASME Journal of Pressure Vessel Technology 99:584–592.

Metzger, D.R., Gagnon, A., Kashyap, T. (2021), *Analysis of Test Method to Extract Material Properties from Candu Fuel Channel Spacers Made of Helical Springs*, Proceedings of the ASME 2021 Pressure Vessels and Piping Conference, Virtual.

Metzger, D.R., Gagnon, A., Kashyap, T., Vidican, R. (2021), *Mechanical Testing Methods Applicable to the Helical Form of Annulus Spacer Components*, 40th Annual Conference of the Canadian Nuclear Society, Virtual.